Natural Frequencies Behavior of a Cantilever Composite Beam with Embedded Shape Memory Alloy Wires

By Dr. Qasim Abbas Atiyah
Department of Mechanical Engineering, University of Technology
Dr_qasim_uot@yahoo.com
Received 17 September 2014 Accepted 25 November 2014

Abstract:
Recently, Shape Memory Alloys (SMAs) has been on the forefront of research. SMAs are unique alloys in that they can remember an original shape after being deformed. They have been used for a wide variety of applications in various fields. The natural frequencies have been identified as one of the most critical parameter in vibration study which may lead to structure failure during resonance. In present work, an analytical solution for the calculation of natural frequencies of composite cantilever beams with embedded SMA wires was studied. The beams were clamped at one end and free in other end. A mathematical model is developed to describe the behavior of the natural frequencies of a cantilever composite beam embedded by SMA wires and solved by using Matlab program. The natural frequencies found from the analytical were compared with previous research and got a good agreement error. It was found that the natural frequencies of beams decreased with increasing the number of embedded SMA wires at a temperature below martensite temperature transformation and increased with increasing the number of embedded SMA wires at a temperature above austenite finish transformation. Some geometrical factors and mechanical properties were studied in this work, such as width of beam, thickness of beam, length of beam, diameters of SMA wires, modulus of elasticity of Glass fiber epoxy, and austenite ratio in SMA wires. Increasing these factors caused increasing in the natural frequencies of composite beam while the increase of length of beam resulted in decreasing in natural frequencies.

Key Words: Composite Beam, Shape Memory Alloy, Vibration Characteristics.

دراسة تصرف الترددات الطبيعية لعتبة حدية مركبة مدعمة بأسلاك سبائك ذاكرة الشكل

م.د قاسم عباس عطية
الجامعة التكنولوجية / قسم الهندسة الميكانيكية

الخلاصة :
تعتبر بحوث سبائك ذاكرة الشكل في مقدمة البحوث الحديثة وذلك بسبب خصائص سبائك ذاكرة الشكل الفريدة من نوعها حيث انها تعود الى شكلها الأصلي بعد تعرضها للتشوه وهذه الميزة جعلتها تستخدم في تطبيقات واسعة ومختلفة. وبسبب كون الترددات الطبيعية واحدة من العوامل المؤثرة على فشل الهياكل نتيجة حدوث الرنين. فقد تم في هذا العمل ايجاد الحل التحليلي لحساب

الترددات الطبيعية لعتبة حدية مصنوعة من مادة مركبة مقواة بأسلاك مصنوعة من سبائك ذاكرة الشكل وهذه العتبة تكون مثبتة من احدى نهايتيها وحرة من النهاية الأخرى وقد تم تطوير الحل تحليلي لايجاد تلك الترددات بأستخدام برنامج ماثلاب. النتائج تم مقارنتها مع أبحاث سابقة واعطت مطابقة جيدة ونسبة خطأ مقبولة. وقد وجد في هذا البحث ان الترددات الطبيعية انخفضت مع زيادة عدد الاسلاك المقواة عند درجة حرارة دون درجة التحول الكلي لطور المارتنسايت وازدادت مع زيادة عدد الاسلاك المدعمة عند درجة حرارة اعلى من درجة التحول الكلي الى طور الاوستنايت. كذلك تمت دراسة بعض العوامل الشكلية والخواص الهندسية مثل عرض العتبة وسمك العتبة وسمك قطر سلك التدعيم لسبائك ذاكرة الشكل ومعامل المرونة لمادة الأساس للالياف الزجاجية ونسبة طور الاوستنايت في اسلاك التدعيم. وقد وجد بان زيادة قيم هذه العوامل يسبب زيادة في قيم الترددات الطبيعية للعتبة. بينما سببت زيادة طول العتبة في تناقص قيم الترددات الطبيعية.

مفاتيح الكلمات: العتبة المركبة ، سبائك ذاكرة الشكل ، خصائص الاهتزازات

Notations:

M_s : Martensite starts temperature upon cooling;
M_f : Martensite finish temperature upon cooling;
A_s : Reverse transformation start temperature upon heating;
A_f : Reverse transformation finish temperature upon heating.
$E_{comp.}$: Modulus Elasticity
$\alpha_{comp.}$: Coefficient of thermal expansion of the composite beam,
$\Theta(\xi)$: The coefficient of the thermal expansion of the SMA wires
E : The tensile modulus.
I : Cross-sectional moment of inertia.
ρ : Mass per unit area.
ω_n: Natural frequency of the beam.

1. Introduction:

SMA possesses an interesting property by which the metal remembers its original size or shape and reverts to it at a characteristic transformation temperature. SMA alloys change phase (between martensite and austenite) at certain critical temperatures, and therefore they display different stress-strain characteristics in different temperature ranges [1]. They attracted much attention in recent years, since they are smart materials, as well as functional materials, which already exist. In the last decade, the development of smart composite materials and structures has become an attractive research topic in an area of materials science and engineering. Smart structures involve embedded smart material actuators as well as microprocessors. The structures are able to respond to external commands or locally change in conditions, with control achieved by actuators applying localized strains or stresses [2].

2. Literature Review:

In recent years, many literatures have reported the use of embedded SMA actuators for composite beams. The embedded SMA actuators could induce an additional bending moment, in order to provide an additional strength to the composite beams. Lau and et al. [3] presented an analytical model for the evaluation of natural frequencies of glass fibre composite beams with embedded shape memory alloy (SMA) wires. The beams were clamped at both ends, and different numbers of SMA actuators were embedded at an interlayer of the composite beams. The authors studied the changes of tensile modulus, internal recovery of stress and strain, and stresses due to the thermal expansion of the beams, wires. They found that the natural frequencies of composite beams decreased with increasing the number of embedded SMA actuators at a temperature below martensite finish temperature and at a temperature above austenite finish temperature. And, the natural frequencies of the beams with low SMA wire fraction initially decreased and then increased with increasing the number of SMA wires.

Lau [4] studied a common type of SMA actuator, Nitinol wires embedded into advanced composite structures to modulate the structural dynamic responses, in terms of natural frequency and damping ratio by using its shape memory and pseudo-elastic properties. He introduced a theoretical model to estimate the natural frequency of the structures before and after actuating the embedded SMA wires and measured the damping ratios of different SMA composite beams through experimental approaches.

Tan et al. [5] studied the fundamental frequency of hybrid composite plate embedded with the SMA wire using impact hammer testing on different boundary conditions. They showed that the results of the fundamental frequency and damping ratio for the hybrid composite plate were shifted and were dependent on the heat level applied to the wires and the boundary conditions of the plate.

Sato et al. [6] investigated the vibration characteristics of symmetric Carbon Fiber Reinforced Plastics (CFRP) laminates with embedded shape memory alloy fibers for passive vibration control by tailoring the laminate configuration. They studied using two in-plane lamination parameters in addition to four out-of-plane lamination parameters, the shape memory effect on the fundamental frequencies for the case of simply supported edges.

Yuvaraja and Senthilkumar [7] studied the vibration control of Glass Fiber Reinforced Plastics (GFRP) flexible composite beam using shape memory alloy (SMA). They measured the tip displacement of the beam to study the extent of vibration control and developed a mathematical model to describe the behavior of the composite.

Birman and Rusnak [8] presented the mathematical formulation of the vibration control mechanism that combines an effective continuous elastic foundation representing the support provided by SMA wires to the structure with the energy dissipation as a result of the hysteresis occurring in the wires. They obtained a closed form expression for the loss factor in large aspect ratio plates supported at the mid-span by a system of parallel SMA wires.

Yuvaraja and Senthilkumar [9] presented the SMA based and PZT based composites for investigating the vibration characteristics. A smart beam consisting of a Glass Fibre Reinforced Polymer (GFRP) beam in cantilevered configuration with externally attached SMAs was modeled. The authors investigated the vibration suppression of smart beam by using ANSYS and evaluated experimentally the vibration control of flexible beam for first mode.

Barzegari et al [10] evaluated the numerical-based analysis for the natural frequencies and mode shapes of the plate with embedded shape memory alloy wires. They modeled plates in according to the classical plate theory (CPT) as well as first-order shear deformation plate theory (FSDT) and SMA wires as a beam. The effect of axial load generated by SMA wires due the change of temperature on the natural frequencies was studied.

Most of the previous researches have not found an exact solution for the cantilever composite beam embedded by SMA wires, and some important factors which effect on the behaviour of the natural frequencies have not studied enough. Therefore, a new calculation approach to find the exact solution for determination the natural frequencies is investigated in this work. Also, some parameters which affected on the vibration properties, such as length of beam, width of beam, thickness of beam, diameter of embedded SMA wires, the ratio of austenite phase in that wires, and modulus of elasticity of Glass fiber epoxy are studied in this research.

3. Theoretical Approach:

Considering the beam shown in Figure (1), the cantilever beam is clamped in one end and free in other end, the SMA wires are embedded into the beam's longitudinal direction, the fourth order differential equation for the lateral vibration of the beam is [3]:

$$EI\frac{d^4y(x)}{dx^4}+F\frac{d^2y(x)}{dx^2}-\rho\omega_n^2y(x)=0 \qquad (1)$$

Where:

$$F_{net} = F_{recovery} - F_{thermal} \quad (2)$$

$$F_{net} = F_{recovery} - (E_{comp}\alpha_{comp}bw + \Theta(\xi))\Delta T \quad (3)$$

The general solution of equation (1) is [4]:

$$y(x) = Acosh(\beta_1 x) + Bsinh(\beta_1 x) + Ccos(\beta_2 x) + Dsin(\beta_2 x) \quad (4)$$

Where:

$$\beta_1 = \left[\left(\frac{F_{net}}{2EI}\right)^2 + \frac{\rho\omega_n^2}{EI}\right]^{0.5} + \frac{F_{net}}{2EI} \quad (5)$$

$$\beta_2 = \left[\left(\frac{F_{net}}{2EI}\right)^2 + \frac{\rho\omega_n^2}{EI}\right]^{0.5} - \frac{F_{net}}{2EI} \quad (6)$$

And:

$$\frac{dy(x)}{dx} = \beta_1[Asinh(\beta_1 x) + Bcosh(\beta_1 x)] - \beta_2[Csin(\beta_2 x) - Dcos(\beta_2 x)] \quad (7)$$

$$\frac{d^2y(x)}{dx^2} = \beta_1^2[Acosh(\beta_1 x) + Bsinh(\beta_1 x)] - \beta_2^2[Ccos(\beta_2 x) + Dsin(\beta_2 x)] \quad (8)$$

$$\frac{d^3y(x)}{dx^3} = \beta_1^3[Asinh(\beta_1 x) + Bcosh(\beta_1 x)] + \beta_2^3[Csin(\beta_2 x) - Dcos(\beta_2 x)] \quad (9)$$

Boundary conditions:

The boundary conditions for cantilever beam are:

1) $y(x) = \frac{dy(x)}{dx} = 0 \quad at\ x = 0$ (i.e. at clamped edge) (10)

2) $\frac{d^2y(x)}{dx^2} = \frac{d^3y(x)}{dx^3} = 0 \quad at\ x = l$ (i.e. at free edge) (11)

From the first boundary conditions:

$$A + C = 0 \ \rightarrow A = -C \quad (12)$$

$$\beta_1 B + \beta_2 D = 0 \ \rightarrow B = -\frac{\beta_2}{\beta_1} \quad (13)$$

And from the second boundary conditions:

$$\beta_1^2[Acosh(\beta_1 l) + Bsinh(\beta_1 l)] - \beta_2^2[Ccos(\beta_2 l) + Dsin(\beta_2 l)] = 0 \quad (14)$$

$$\beta_1^3[Asinh(\beta_1 l) + Bcosh(\beta_1 l)] + \beta_2^3[Csin(\beta_2 l) - Dcos(\beta_2 l)] = 0 \quad (15)$$

But eqs. (12) & (13) in eqs. (14) & (15) get:

$$\beta_1^2[A cosh(\beta_1 l) + B sinh(\beta_1 l)] + \beta_2^2\left[A cos(\beta_2 l) + \frac{\beta_1}{\beta_2} B sin(\beta_2 l)\right] = 0 \tag{16}$$

$$\beta_1^3[A sinh(\beta_1 l) + B cosh(\beta_1 l)] - \beta_2^3\left[A sin(\beta_2 l) - \frac{\beta_1}{\beta_2} B cos(\beta_2 l)\right] = 0 \tag{17}$$

Re-arranging eqs. (16) & (17)

$$A(\beta_1^2 cosh(\beta_1 l) + \beta_2^2 cos(\beta_2 l)) + B(\beta_1^2 sinh(\beta_1 l) + \beta_1\beta_2 sin(\beta_2 l)) = 0 \tag{18}$$

$$A(\beta_1^3 sinh(\beta_1 l) - \beta_2^3 sin(\beta_2 l)) + B(\beta_1^3 cosh(\beta_1 l) + \beta_2^2\beta_1 cos(\beta_2 l)) = 0 \tag{19}$$

i.e., eqs. (18) & (19) can be written in matrix form:

$$\begin{vmatrix} (\beta_1^2 cosh(\beta_1 l) + \beta_2^2 cos(\beta_2 l)) & (\beta_1^2 sinh(\beta_1 l) + \beta_1\beta_2 sin(\beta_2 l)) \\ (\beta_1^3 sinh(\beta_1 l) - \beta_2^3 sin(\beta_2 l)) & (\beta_1^3 cosh(\beta_1 l) + \beta_2^2\beta_1 cos(\beta_2 l)) \end{vmatrix} \begin{bmatrix} A \\ B \end{bmatrix} = \begin{bmatrix} 0 \\ 0 \end{bmatrix} \tag{20}$$

The phase transformation tensor Ω can be expressed as functions detail expression of the relationship of the martensite fraction ξ and applied temperature, T for the martensitic transformations.

$$\xi = \frac{\xi_M}{2}\{cos[a_A(T - A_S)] + 1\} \tag{21}$$

$$\xi = \frac{1-\xi_A}{2}\left\{cos[a_M(T - M_S)] + \frac{1+\xi_A}{2}\right\} \tag{22}$$

The tensile modulus and coefficient of thermal expansion of the SMA materials can be evaluated by using the mixture law, i.e.,

$$D(\xi) = \xi D_M + (1 - \xi) D_A \tag{23}$$

$$\Theta(\xi) = \xi\Theta_M + (1 - \xi)\Theta_A \tag{24}$$

The modulus and density can be determined as follow:

$$E = E_1 + [D(\xi) - E_1]\frac{A_{SMA}}{A_{total}} \tag{25}$$

$$\rho = \rho_c + [\rho_{SMA} - \rho_c]\frac{A_{SMA}}{A_{total}} \tag{26}$$

The natural frequency of the composite cantilever beam embedded by SMA wires can be determined by solving the above matrices, the general forms of solutions after considering the boundary conditions in equations (10) & (8), the analytical solutions for evaluating the natural frequency of the composite beams, are [11]:

$$\omega_n = \left(\frac{2n-1}{2}\pi + e_n\right)^2 \frac{1}{L^2}\sqrt{\frac{EI}{\rho A}} \quad , \quad n = 1,2,.,.,.,.\infty \tag{27}$$

Where e_n are small correction terms, and obtianed as:
$e_1 = 0.3042$

$e_2 = -0.018$
$e_3 = 0.001, ., ., .,$
The correction in the higher modes tend to zero rapidly, and can be neglected.

4. Results and discussions:

In the present work, NiTicCu and Glass fiber epoxy are used as SMA wires and composite beam material respectivelly. The mechanical properties of SMA material and epoxy are illustrated in table (1).
The dimensions of samples are listed in table (2), these samples are used for comparsion between the present numeircal results and results of ref. [4], as shown in table (3). this table shows a good agreement between present results and experimential results of ref. [4], espically in samples Beam-3WM, Beam-5WM, and Beam-3WA, the error in these samples is less than 1%. Also, there is a small error is between present results and numerical results of ref. [4], especially in samples Beam-1WM, Beam-3WM, Beam-5WM, Beam-3WA, and Beam-5WA.
Figures (2), (3) & (4) show the behavior of changing the natural frequencies with no. of embedded wires in composite beam at two cases, first in SMA wires fully in martensite phase (i.e., $T < M_f$) and second in SMA wires fully in austenite phase (i.e., $T > A_f$). In these figures, the values of natural frequencies in all modes decreased when the number of SMA wires incresed in martensite phase transformation, and the natural frequencies increased when the number of SMA wires increased. The first three natural frequencies decreased by 5.759% when the embedded SMA wires increased from one wire to 19 wires in martensite phase, and the first three natural frequencies increased by 2.129% when the embedded SMA wires increased from one wire to 19 wires in austenite phase. Figure (5) depicts the relation between the natural frequencies of composite material and length of beam. The behaviour of changing in the first three modes is logarithmic, when the length increased from 200 to 440 mm, the first three natural frequencies decreased by 79.338%.
The relation between the width of beam and values of natural frequencies is shown in figure (6). In this figure, when width increased, the values of natural frequencies in all modes are increased too. The natural frequencies increased by 2.09% when the width increased from 20 mm to 40 mm.
Figure (7) manifests the relation between the thickness of beam and values of natural frequencies, this figure shows when the thickness of beam is increased, the natural frequencies highly increased, therefore the values of natural frequencies increased by 157.42% when the thickness is just increased from 1 mm to 2.5 mm. The relation between the diameters of SMA wires with natural frequencies is clarified in figure (8). In this figure, when the diameter is increased, the values of natural frequencies of embedded composite beam decreased. The natural frequencies decreased by 14.45% when the diameter of embedded wired is increased from 5 mm to 15 mm.
Figure (9) shows the relation between the austenite phase ratio in composite beam in embedded wires of SMA and the values of natural frequencies of beam, the value of temperature in beam controls this ratio of austenite phase, when this ratio is increased, the natural frequencies increased. Therefore, the natural frequencies increased by 5.03% when the austenite ratio is increased from 0% to 100% in embedded SMA wires in composite beam. Finally, the relation between the stiffness of composite beam and natural frequencies is illustrated in figure (10). In this figure, when the stiffness of the Glass fiber epoxy of composite beam is increased, the natural frequencies increased. The value of natural frequencies increased by 66.04% when the value of stiffness is increased from 10 GPa to 30 GPa.

5. Conclusions:

In the present work, a numerical solution for the natural frequencies of composite beam embedded by SMA wires is evaluated. Good agreement errors with pervious experimental and numerical results are found. The natural frequencies of beams decreased with increasing the number of embedded SMA wires at a temperature below martensite temperature transformation and increased with increasing the number of embedded SMA wires at a temperature above austenite finish transformation. The increasing in the width of beam, thickness of beam, diameters of SMA wires, modulus of elasticity of Glass fiber epoxy, and austenite ratio in SMA wires caused an increase in the natural frequencies of composite cantilever beam. The increase in the length of beam resulted in a decrease in natural frequencies of beam.

References:

1) M. Senthilkumar, 'Analysis of SMA Actuated Plain Flap Wing', J. of Eng. Science and Technology Review, 2012, Vol. 5, Pp. 39-43.

2) Kazuhiro Otsuka and Xiaobing Ren**, '**Recent Developments in the Research of Shape Memory Alloys', Elsevier, Intermetallics, Vol. 7, 1999, Pp. 511-528.

3) Kin-tak Lau, 'Vibration Characteristics of SMA Composite Beams with Different Boundary Conditions', Elsevier, Materials and Design, Vol. 23, 2002, Pp. 741–749.

4) Kin-tak Lau, Li-min Zhou, and Xiao-ming Tao, ' Control of Natural Frequencies of a Clamped–Clamped Composite Beam with Embedded Shape Memory Alloy Wires', Elsevier, Composite Structures, Vol. 58, 2002, Pp. 39–47.

5) W. Tan, S. Jamian, M. Ghazali and N. Mohamed, 'Fundamental Frequency oF Hybrid Composite Plate Embedded with Shape Memory Alloy Wire ', Computational and Experimental Mechanics, 2007, Pp. 286-294.

6) Masaki Sato, Hideki Sekine, and Yuichi Hayakawa, ' Vibration Characteristics of CFRP Laminates with Embedded Shape Memory Alloy Fibers', Department of Aeronautics and Space Engineering, Tohoku University, 2009.

7) M. Yuvaraja, and M. Senthilkumar, ' Vibration Control of GFRP Composite Beam Using SMA-Flexional Actuators', International J. of Eng. Vol. 8, 2010, Pp. 289-295.

8) Victor Birman and Ian Rusnak,' Vibrations of Plates with Super Elastic Shape Memory Alloy Wires ', J. Eng. Math., 2011.

9) M. Yuvaraja and M. Senthilkumar, 'Comparative Study on Vibration Characteristics of a Flexible GFRP Composite Beam Using SMA and PZT Actuators', Manuf. and Ind. Eng., Vol. 11, 2012, Pp. 28-33.

10) M. Barzegari1, M. Dardel, A. Fathi1, M. Pashaei, 'Effect of Shape Memory Alloy Wires on Natural Frequency of Plates', J. of Mechanical Eng. and Automation, Vol. 2, 2012, Pp. 23-28.

11) P. Hagedorn and A. Dasgupta, 'Vibration and Waves in Continuous Mechanical Systems', John Wiley and Sons Ltd, First edition, 2007.

Table (1): The mechanical properties of SMA material and epoxy [3]

Description	Properties	Type	Value
NiTi (Nitional)	Tensile Modulus	Martensitic Phase	25 GPa
		Austenitic Phace	50 GPa
	Thermal Coefficient		0.55 MPa/^{o}C
	Density		6450 Kg/m^3
	Transformation Temperature	Martensite Finish	25 ^{o}C
		Martensite Start	40 ^{o}C
		Austenitie Finish	55 ^{o}C
		Austenitie Start	48 ^{o}C
Glass Fiber / Epoxy Composite	Tensile Modulus, E_1		12 GPa
	Density		1800 Kg/m^3

Table (2): Description of Testing Samples [4]

Samples	Temp. (^{o}C)	No. of wires	Width (mm)	Length (mm)	Thickness (mm)
Beam	$< M_f$	0	33.2	200	1.41
Beam-1WM	$< M_f$	1	33.1	200	1.44
Beam-3WM	$< M_f$	3	33.4	200	1.51
Beam-5WM	$< M_f$	5	33.3	200	1.50
Beam-1WA	$> A_f$	1	32.3	200	1.40
Beam-3WA	$> A_f$	3	33.0	200	1.44
Beam-5WA	$> A_f$	5	33.3	200	1.50

Table (3): Comparison between present results and Experimental and Numerical results of ref. [4]

Samples	Present results	Numerical results [4]	Experimental results [4]	Errors% with Num.	Errors % with Exp.
Beam	92.37907	97.22	98.63	5.24029%	6.76661%
Beam-1WM	94.05561	96.78	98.12	2.89657%	4.32126%
Beam-3WM	98.08562	96.12	98.10	2.003981%	0.01466%

Beam-5WM	96.88659	95.23	97.56	1.709822%	0.69505%
Beam-1WA	91.83875	71.00	81.8	22.69058%	10.93084%
Beam-3WA	94.67465	91.00	95.5	3.881343%	0.87178%
Beam-5WA	98.81051	97.80	-	1.022673%	-

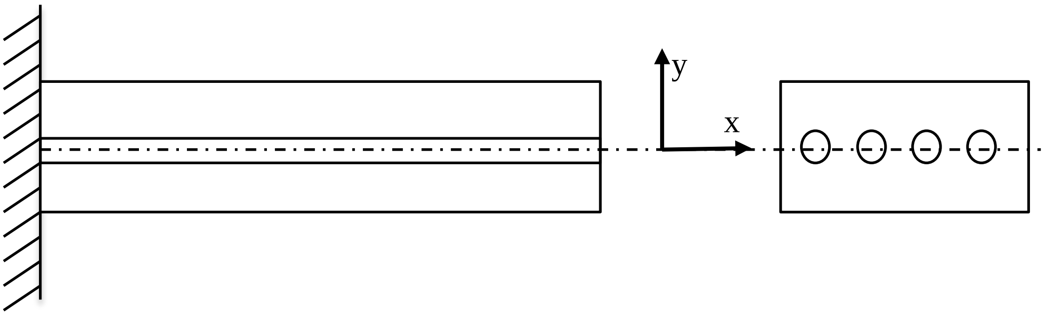

Figure (1): A schematic illustration of the composite beam embedded by SMA wires

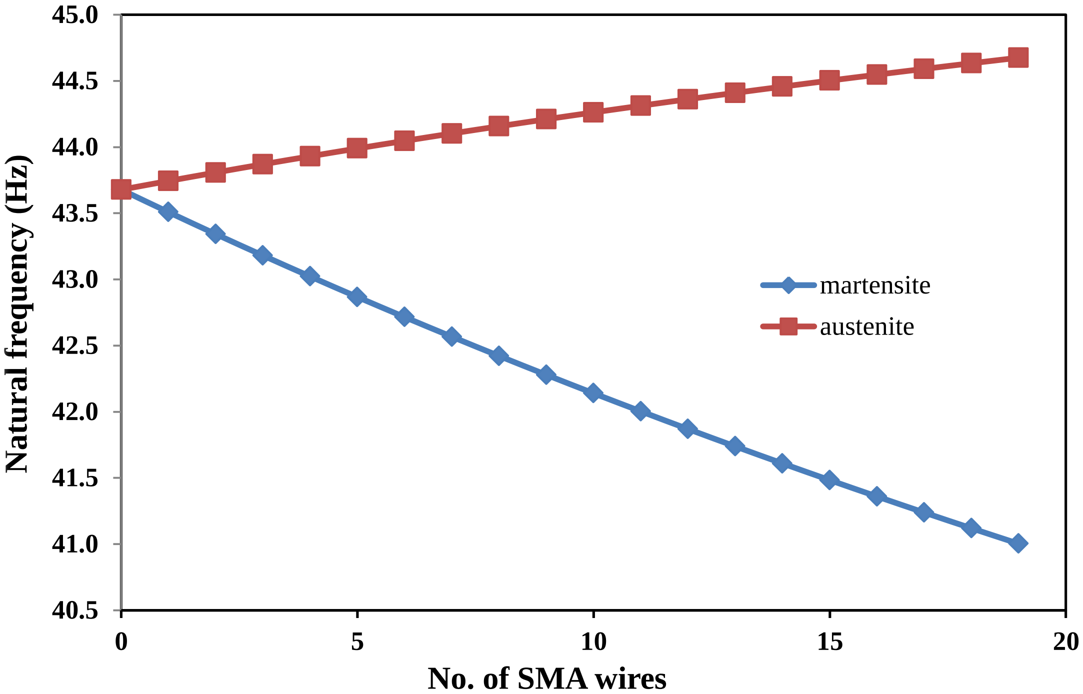

Figure (2): No. of embedded wires vs first natural frequency.

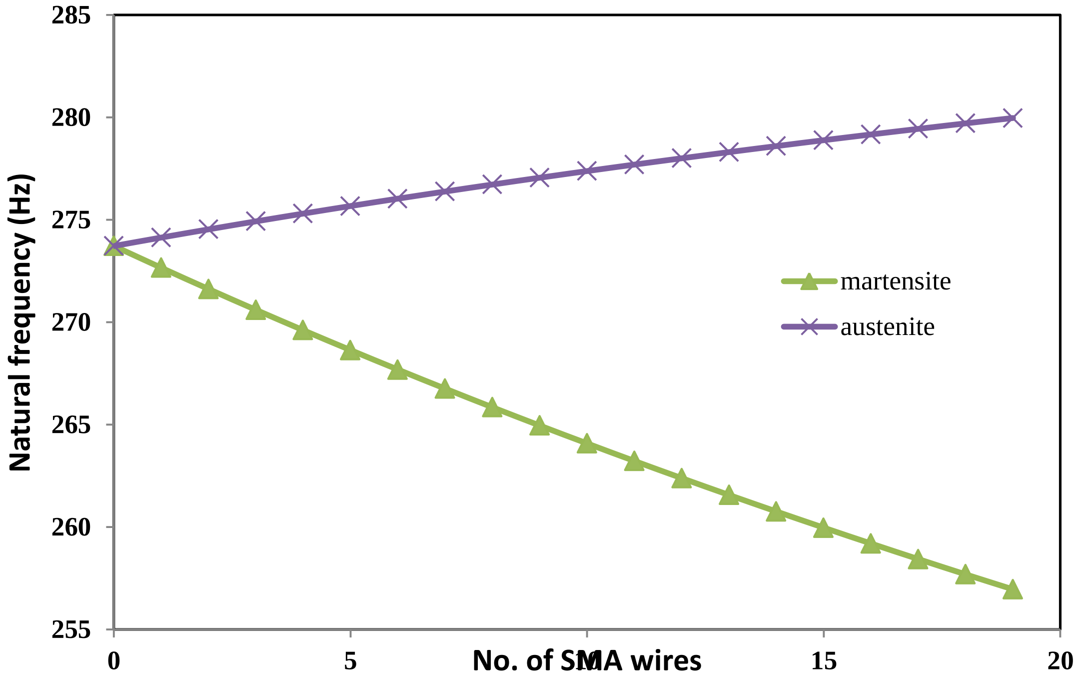

Figure (3): No. of embedded wires vs second natural frequency.

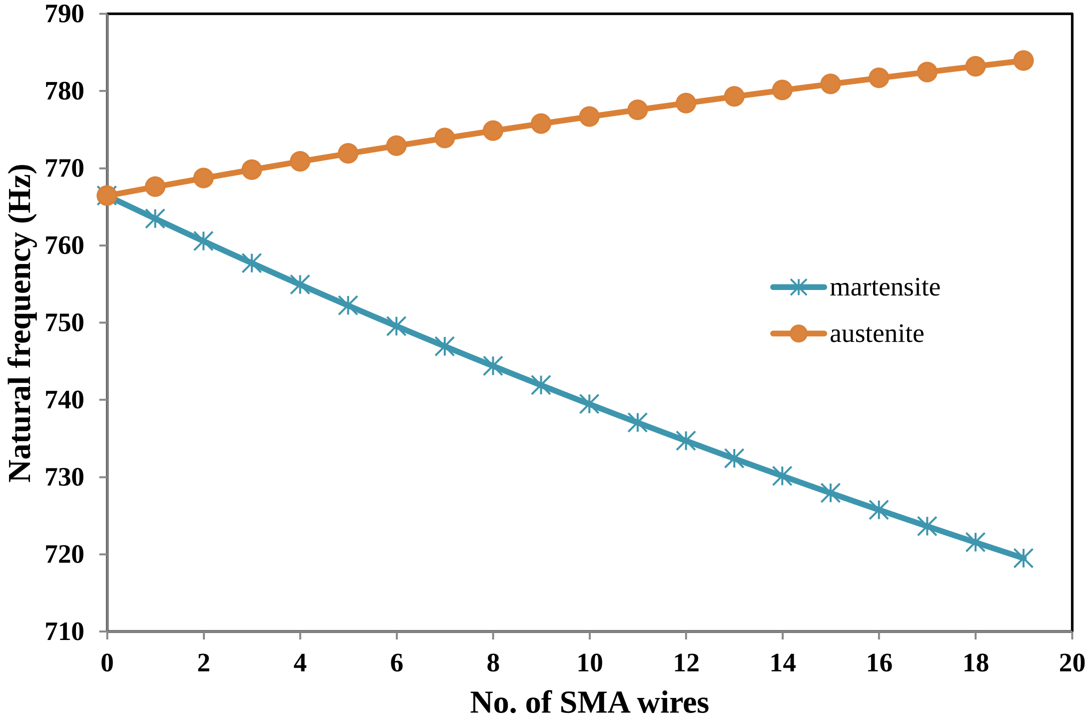

Figure (4): No. of embedded wires vs third natural frequency.

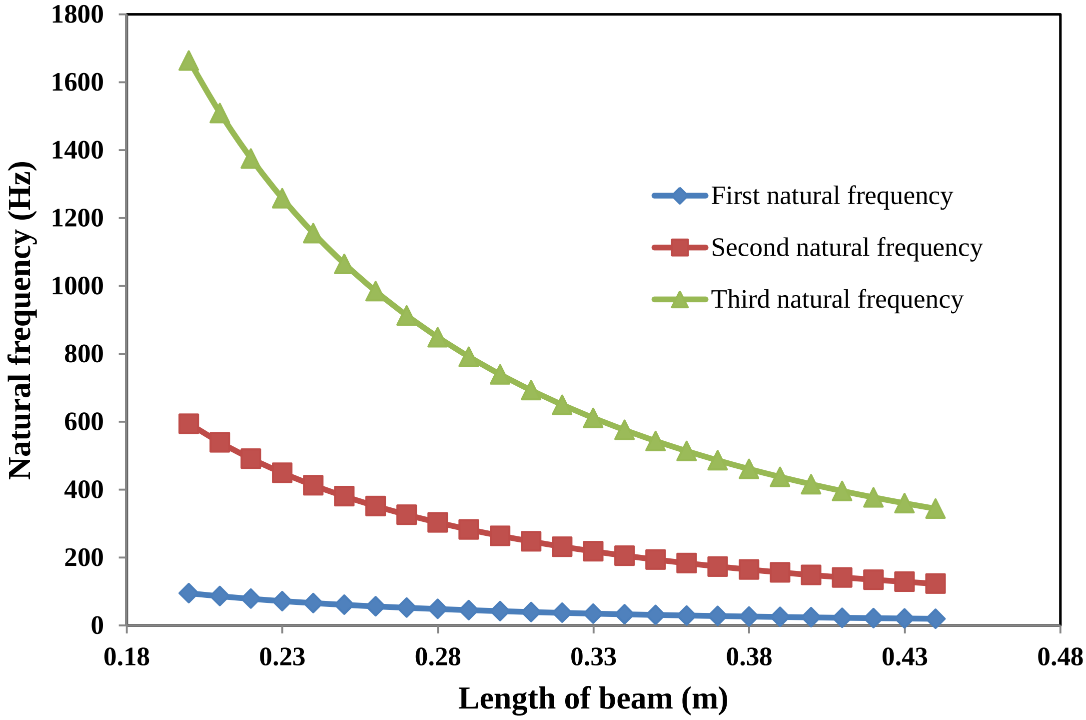

Figure (5): Length of beam vs natural frequency.

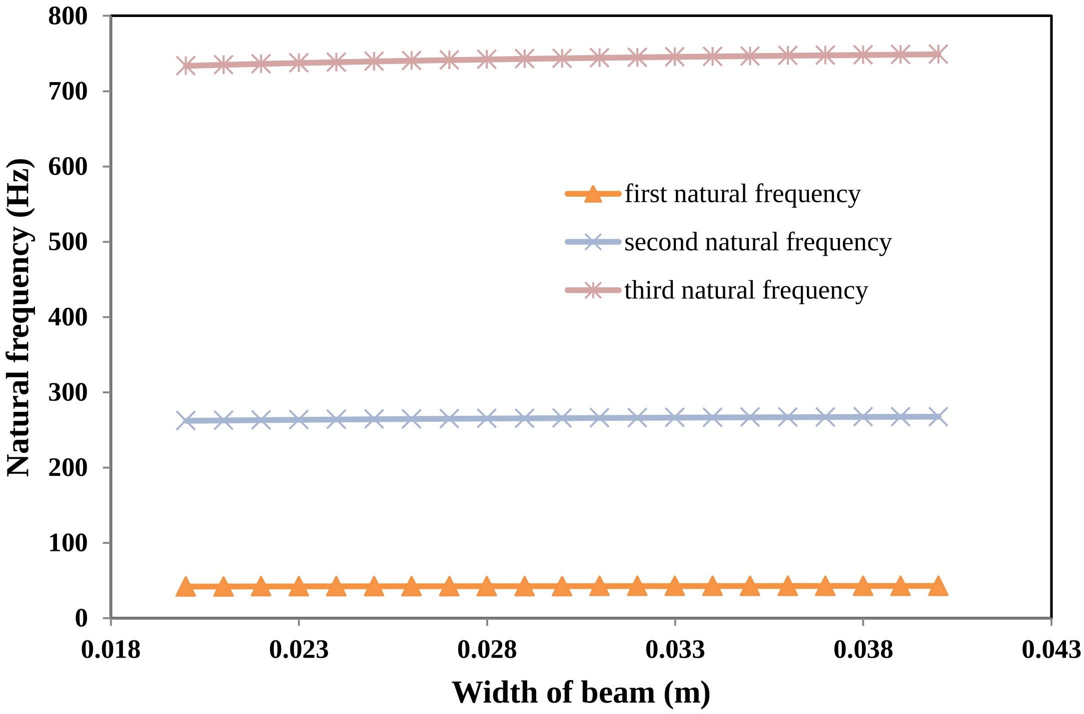

Figure (6): Width of beam vs natural frequency.

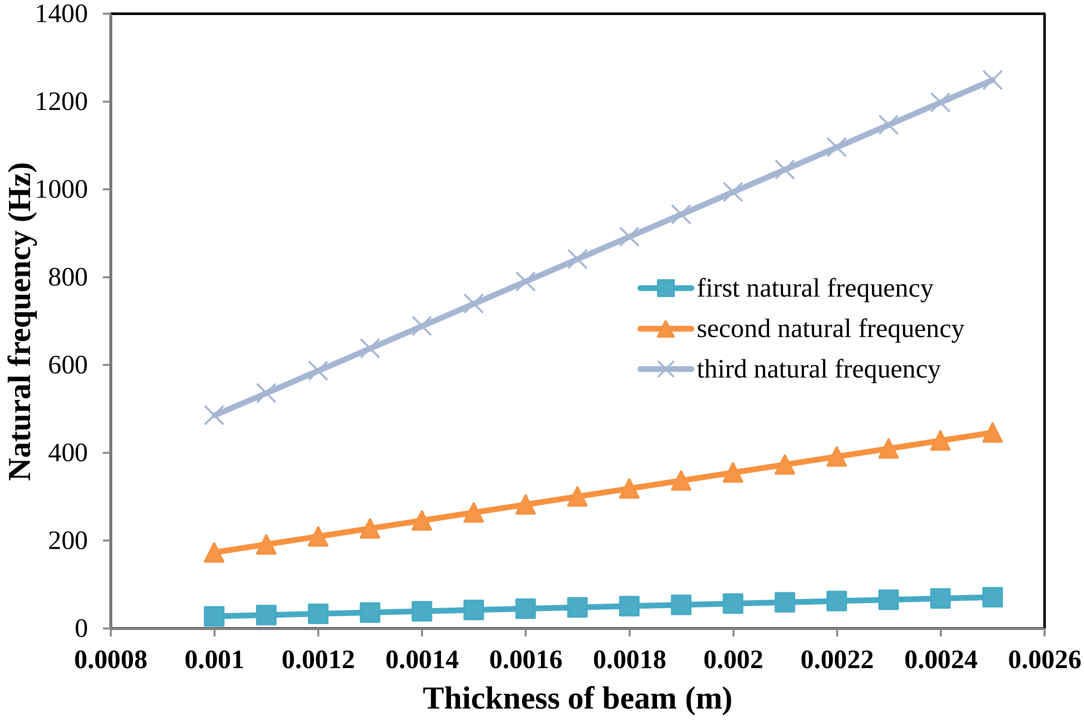

Figure (7): Thickness of beam vs natural frequency.

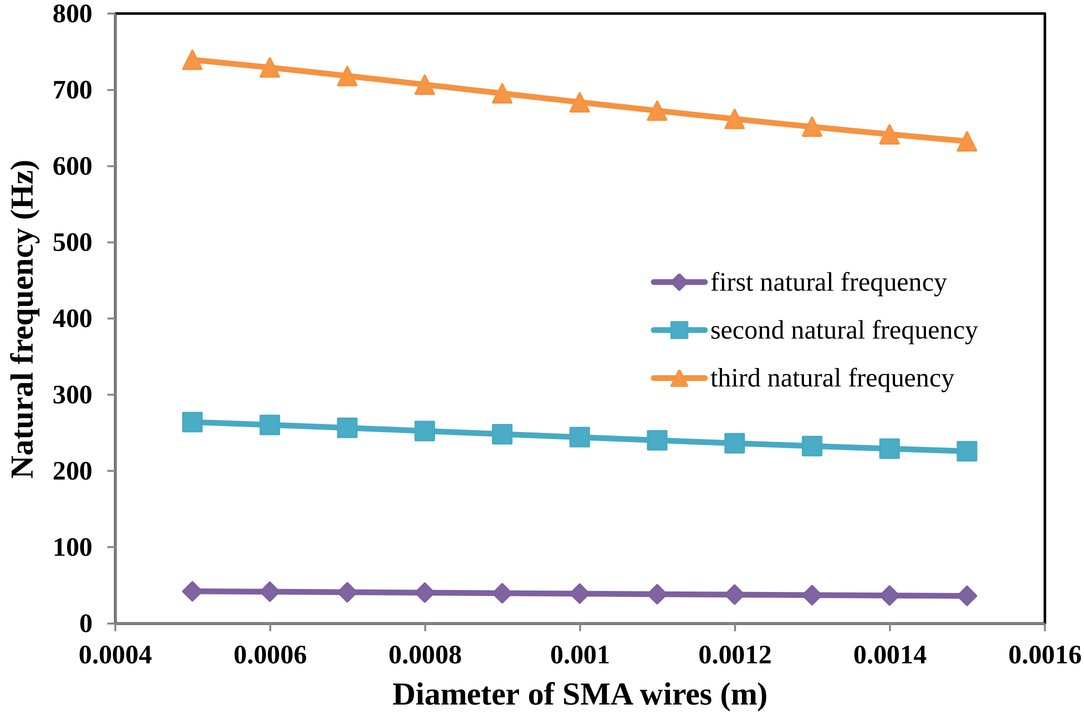

Figure (8): Diameter of SMA wires vs natural frequency.

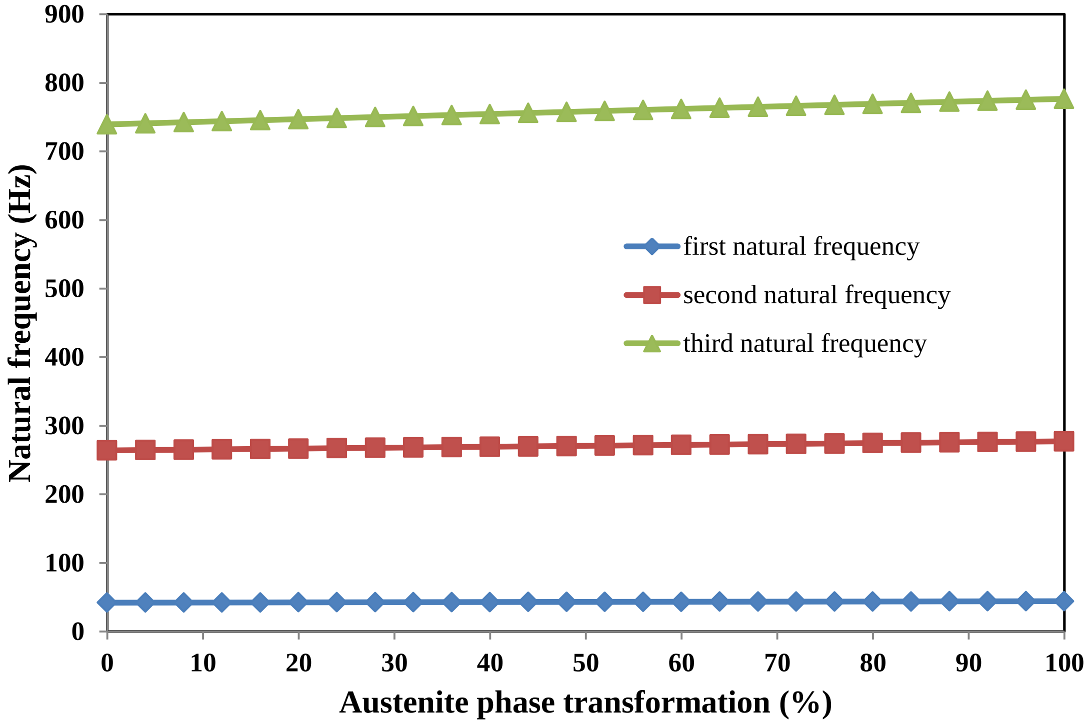

Figure (9): Austenite phase transformation vs natural frequency.

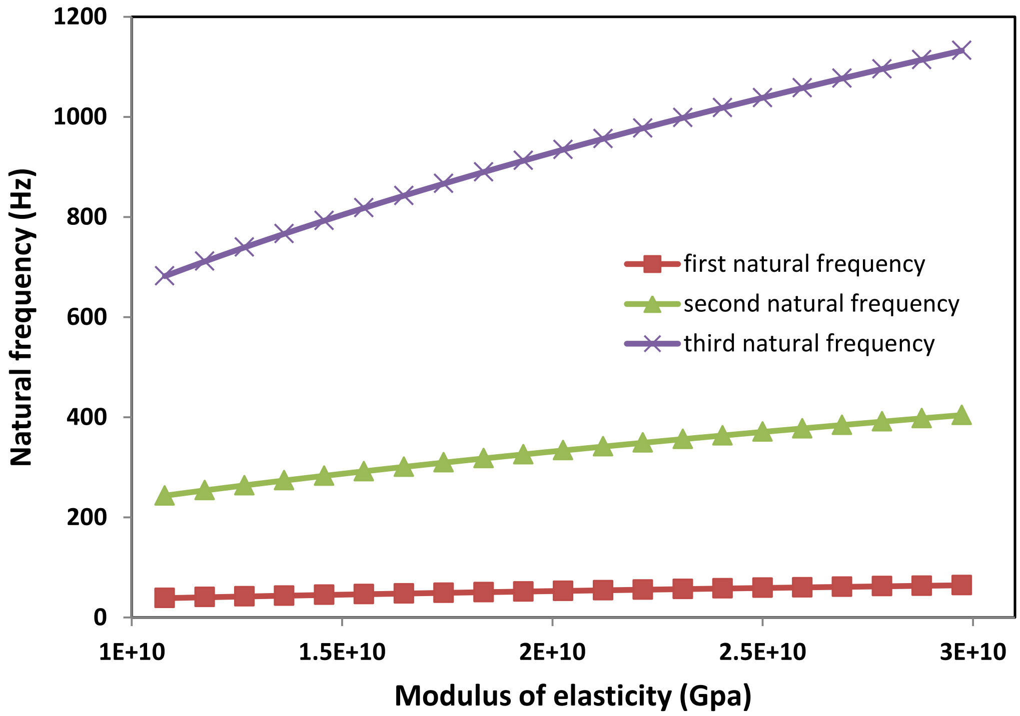

Figure (10): Modulus of elasticity vs natural frequency.